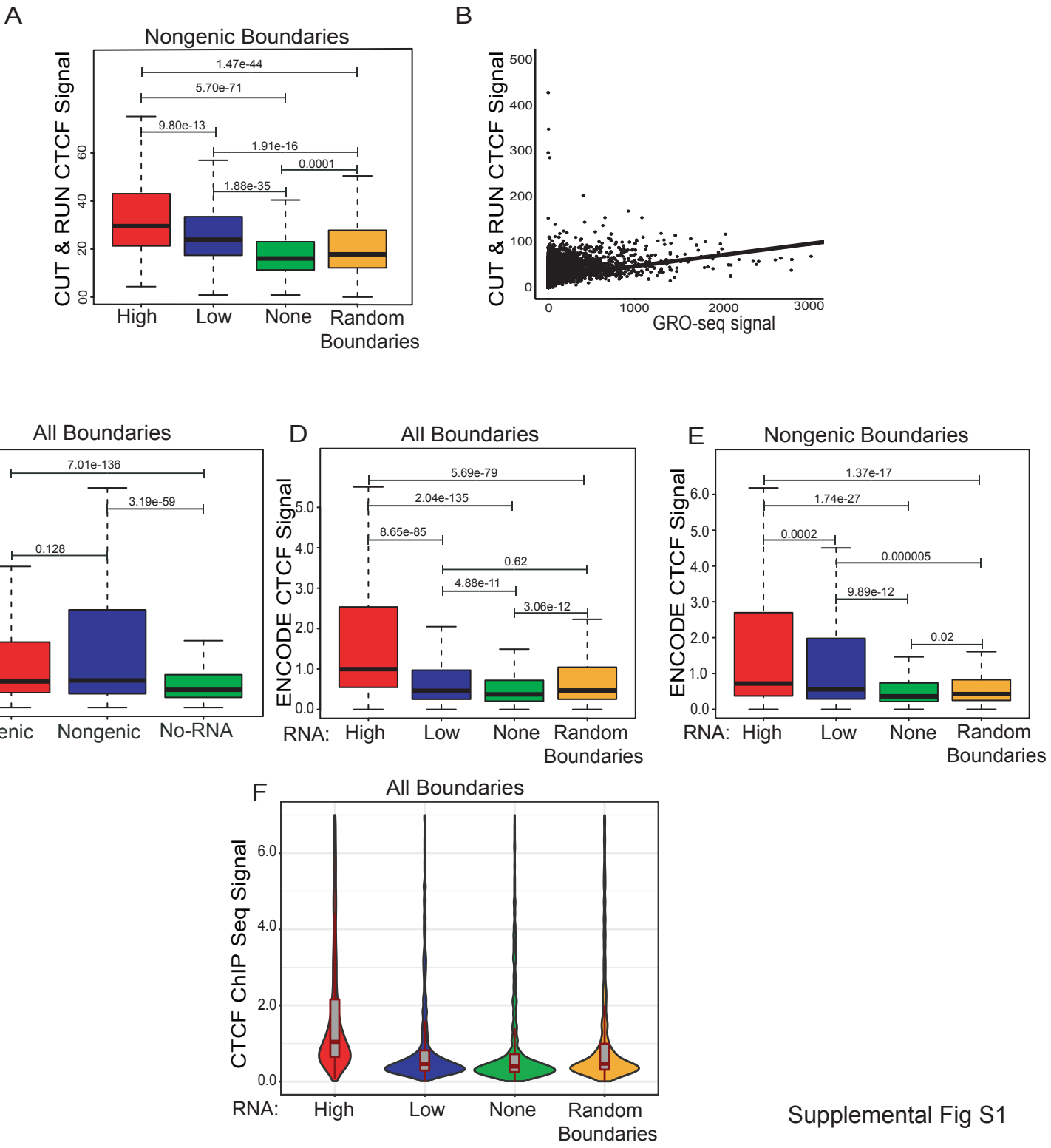

Supplemental Fig S1

Supplemental Fig S1. Transcribed boundaries exhibit better insulation: A. CTCF enrichment (CTCF CUT&RUN) at nongenic transcribed boundaries with high, low RNA versus non-transcribed and random boundaries **B.** levels of RNA and CTCF occupancy at TAD boundaries are positively correlated. **C.** CTCF enrichment (ChIP-seq) at transcribed genic, nongenic and non-transcribed boundaries. **D.** CTCF enrichment at all transcribed boundaries with high, low RNA versus non-transcribed and random boundaries. **E.** CTCF enrichment at nongenic transcribed boundaries with high, low non-coding RNA versus non-transcribed and random boundaries. **F.** Violin plots showing CTCF enrichment on all boundaries exhibiting varying levels of RNAs versus non-transcribed and random boundaries. p-values in boxplots were calculated by the Wilcoxon rank-sum test. The boxplots depict the minimum (Q1-1.5×IQR), first quartile, median, third quartile and maximum (Q3+1.5×IQR) without outliers.

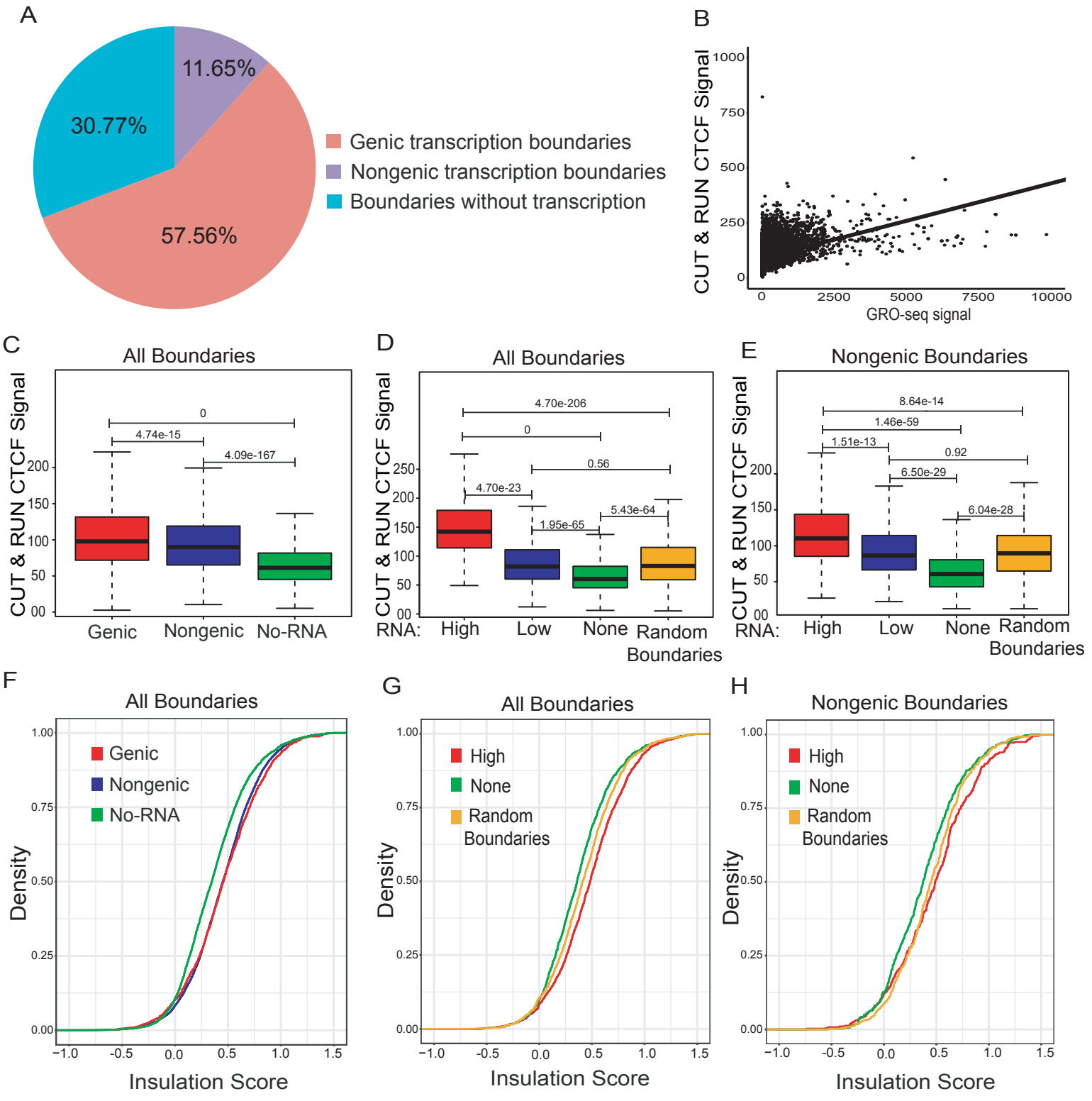

Supplemental Fig S2

Supplemental Fig S2. boundaries defined at 20 kb resolution show the similar features as at 5 kb resolution: A. Pie chart displaying the percentage of boundaries that show genic and nongenic transcribed boundaries and not transcribed boundaries. **B.** Levels of RNA and CTCF occupancy at TAD boundaries are positively correlated. **C.** CTCF enrichment on transcribed genic, nongenic and non-transcribed boundaries. **D.** CTCF enrichment on all transcribed boundaries with high and low RNA versus non-transcribed and random boundaries. **E.** CTCF enrichment on nongenic transcribed boundaries with high and low non-coding RNA versus non-transcribed and random boundaries. **F.** Density plot showing insulation scores for transcribed genic, nongenic and non-transcribed boundaries. **G.** Density plot showing insulation scores for all transcribed boundaries exhibiting varying levels of RNA vs. non-transcribed and random boundaries. **H.** Density plot showing insulation scores of nongenic transcribed boundaries exhibiting varying levels of RNA versus non-transcribed and random boundaries. p-values in boxplots were calculated by Wilcoxon rank-sum test. The boxplots depict the minimum (Q1-1.5×IQR), first quartile, median, third quartile and maximum (Q3+1.5×IQR) without outliers.

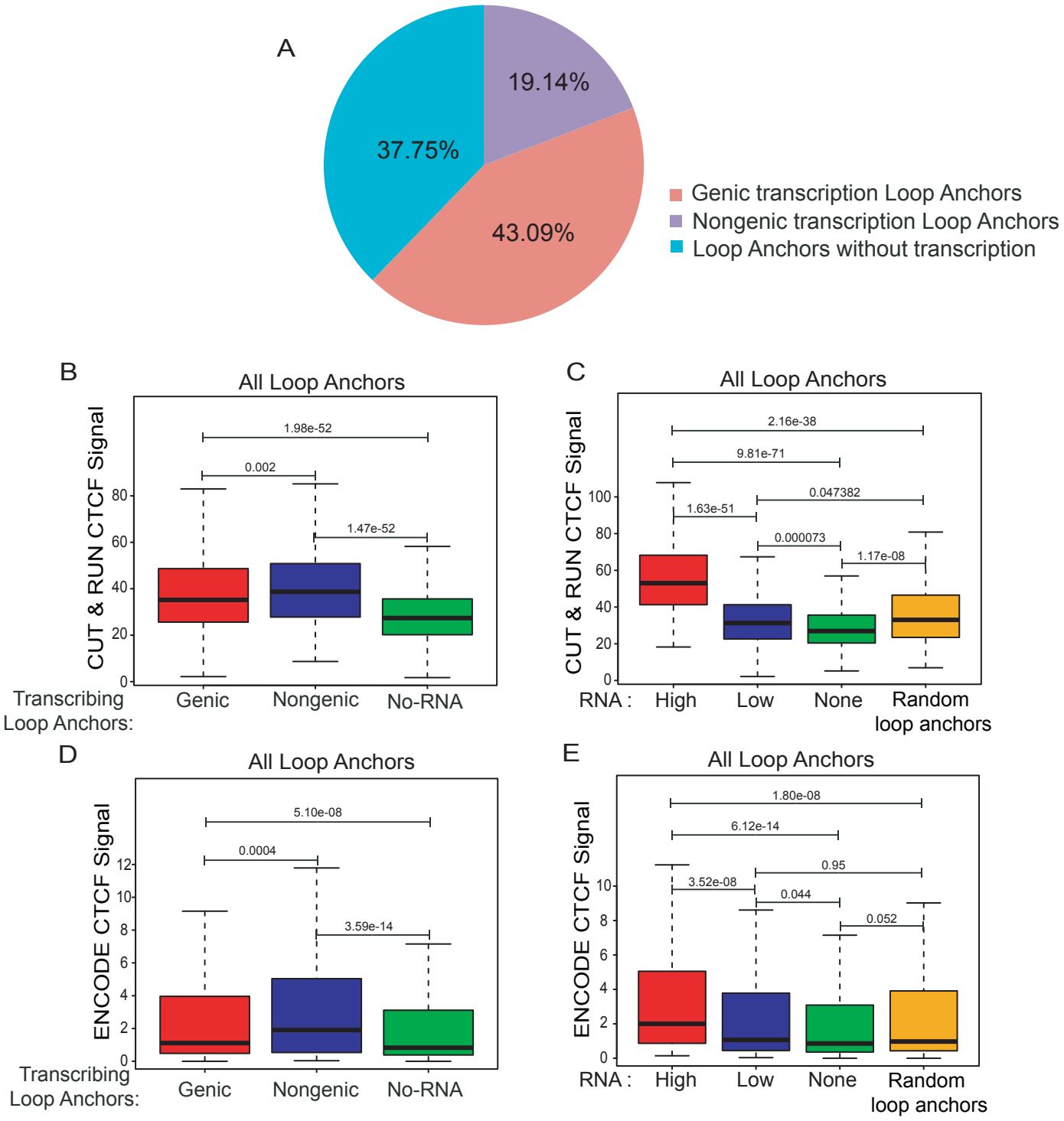

Supplemental Fig S3

Supplemental Fig S3. Transcribed Loop Anchors exhibit more CTCF enrichment: A. Pie chart showing the percentage of loop anchors that overlap with regions of genic transcription and nongenic de novo transcription and regions without transcription. **B.** CTCF enrichment (CTCF CUT&RUN) at transcribed genic, nongenic and non-transcribed loop anchors. **C.** CTCF enrichment on all transcribed loop anchors with high and low RNA versus non-transcribed and random loop anchors. **D.** CTCF enrichment (CTCF ChIP-seq) at transcribed genic, nongenic and non-transcribed loop anchors. **E.** CTCF enrichment at all transcribed loop anchors with high and low RNA versus non-transcribed and random loop anchors. p-values in boxplots were calculated by Wilcoxon rank-sum test. The boxplots depict the minimum (Q1-1.5×IQR), first quartile, median, third quartile and maximum (Q3+1.5×IQR) without outliers.

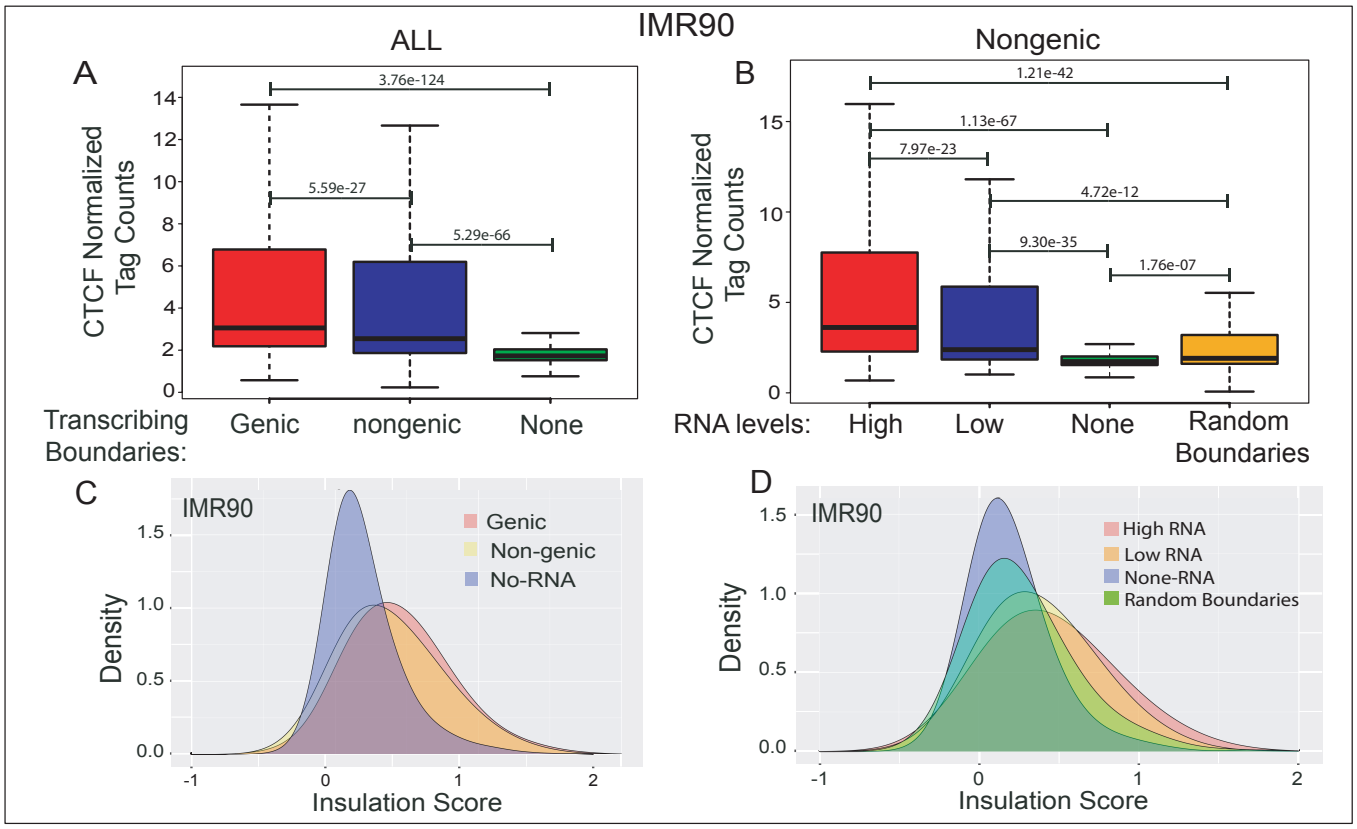

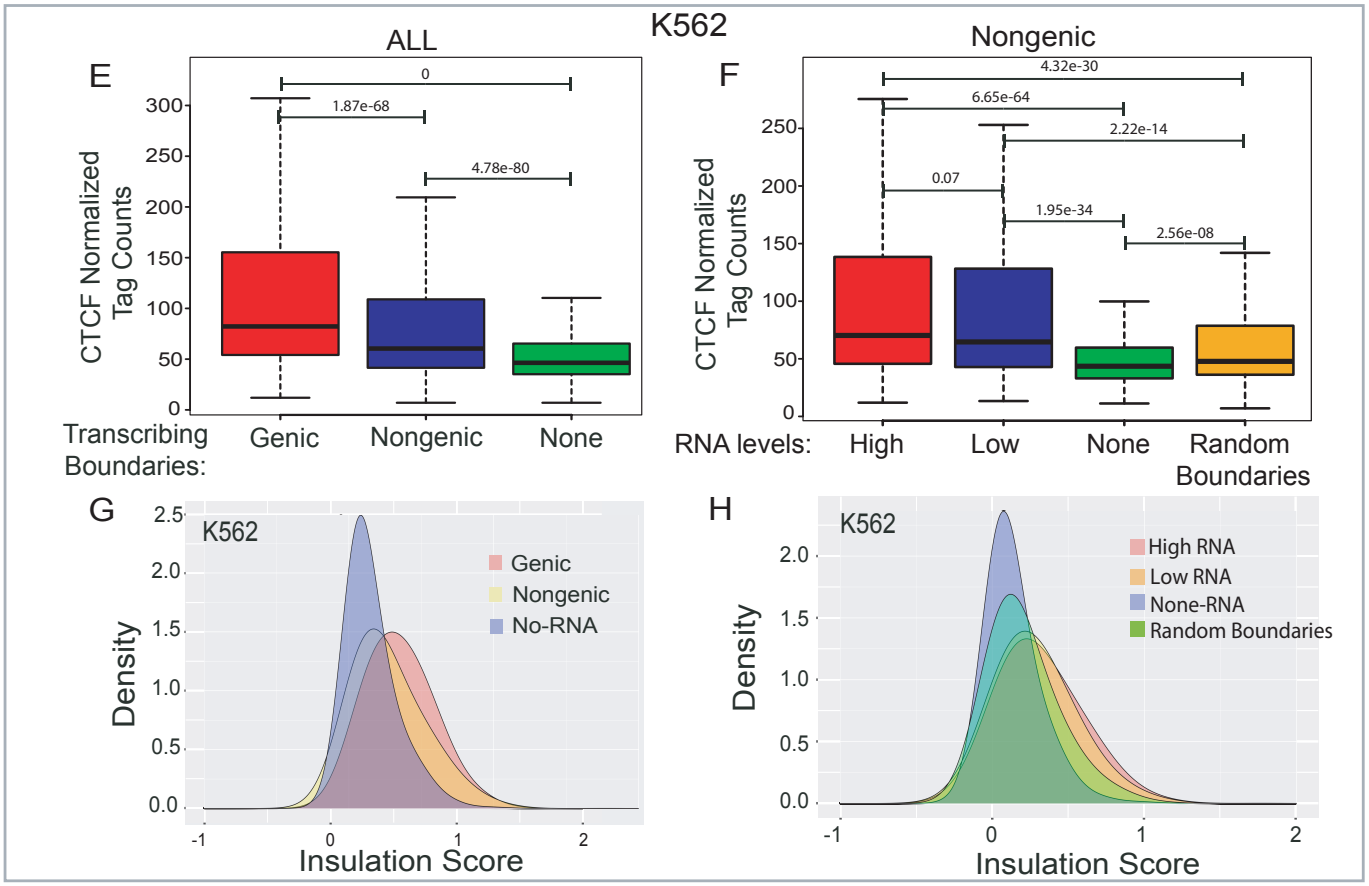

Supplemental Fig S4

Supplemental Fig S4. Transcribed boundaries in IMR-90 and K562 exhibit better insulation: A. CTCF enrichment at transcribed genic, nongenic and non-transcribed boundaries in IMR-90 cells. **B.** CTCF enrichment at nongenic transcribed boundaries with high and low non-coding RNA versus non-transcribed and random boundaries in IMR-90 cells. **C.** Density plots showing insulation scores for transcribed genic, nongenic and non-transcribed boundaries in IMR-90 cells**. D.** Density plots showing insulation scores for nongenic transcribed boundaries exhibiting varying levels of non-coding RNAs versus non-transcribed and random boundaries in IMR-90. **E-F**. Same as A-B in K562 cells. **G-H.** Same as C-D in K562 cells. p-values in boxplots were calculated by Wilcoxon rank-sum test. The boxplots depict the minimum (Q1-1.5×IQR), first quartile, median, third quartile and maximum (Q3+1.5×IQR) without outliers.

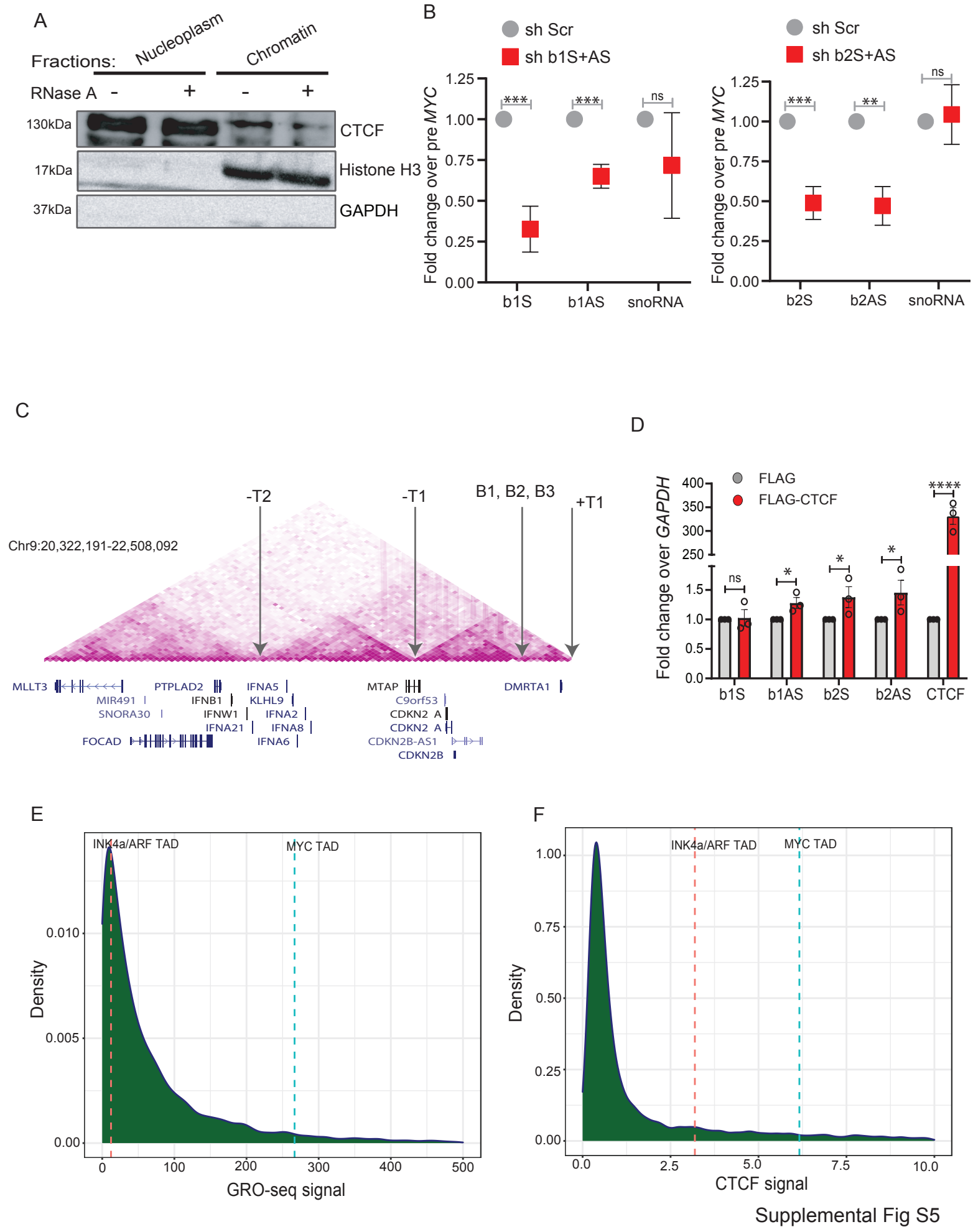

Supplemental Fig S5

Supplemental Fig S5. RNA increases CTCF occupancy at TAD boundary: A. Immunoblotting with CTCF, Histone H3 and GAPDH on soluble nucleoplasm and chromatin-bound fractions of nuclei treated with or without RNase A. **B.** qRT-PCRs showing the levels of sense and anti-sense non-coding RNA at B1and B2 CTCF sites and of snoRNA upon B1 and B2 RNA knockdown in the chromatin associated RNA fraction. **C.** TADs around the *INK4a/ARF* TAD. Positions of arrows show the CTCF sites at upstream and downstream TAD boundaries where CTCF occupancy was interrogated. **D.** qRT-PCRs showing the fold-change in sense and anti-sense RNAs from B1 and B2 CTCF sites upon Flag-CTCF overexpression. The last two bars show the increase in CTCF levels. **E.** Population density distributions of GRO-seq in all transcribing boundaries and indicating where the *INK4a/ARF* (red) and *MYC* TAD(blue) boundaries fall. **F.** Population density distributions of CTCF signal in all transcribing boundaries and indicating where the *INK4a/ARF* (red) and *MYC* TAD(blue) boundaries fall. Error bars denote SEM from three biological replicates. p-values were calculated by Student's two-tailed unpaired *t*-test in **B** and **D**. ****$p < 0.0001$, ***$p < 0.001$, **$p < 0.01$, *$p < 0.05$, $^{ns}p > 0.05$.

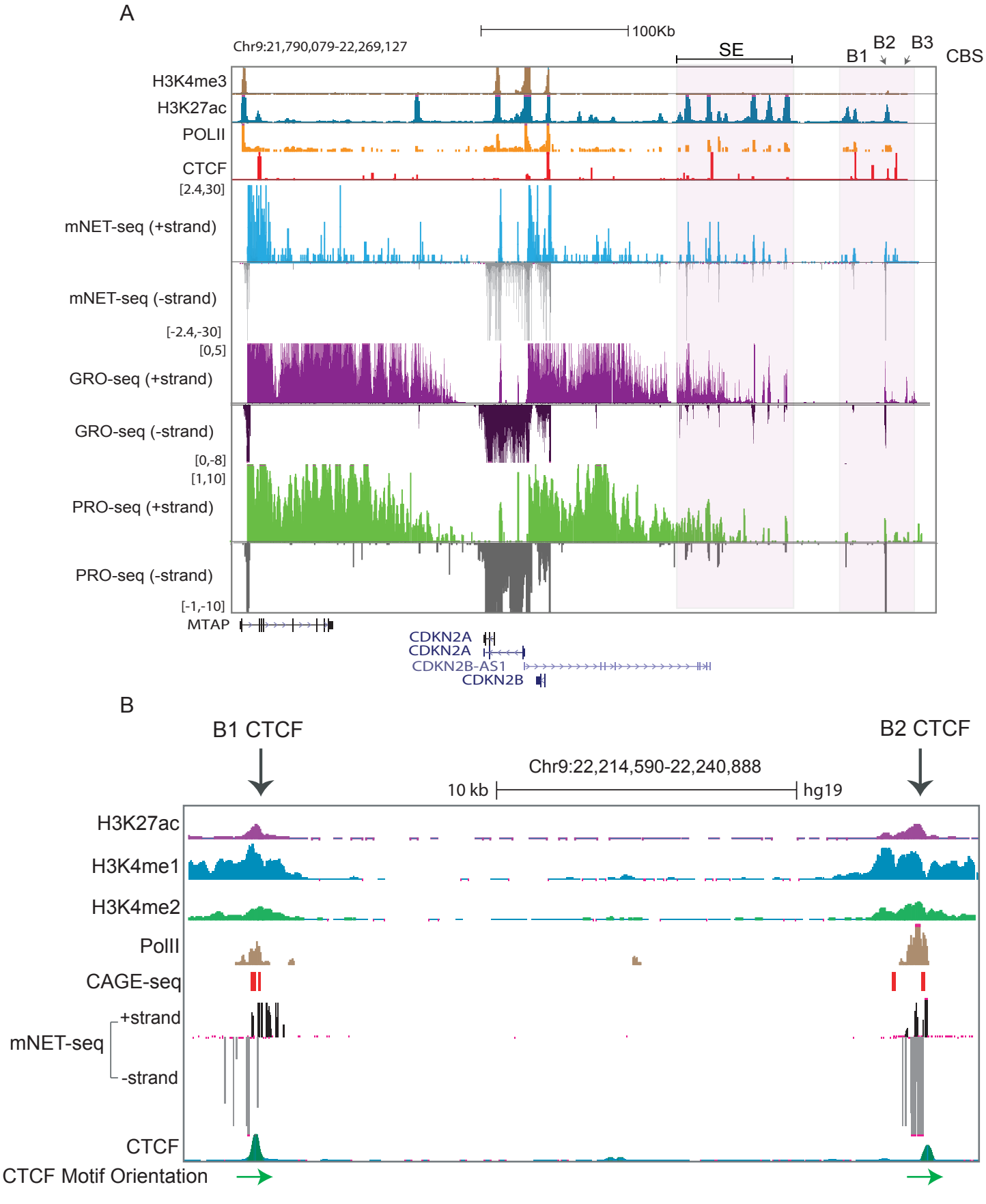

Supplemental Fig S6

Supplemental Fig S6. Browser shots of the *INK4a/ARF* loop domain: A. A browser shot showing the *INK4a/ARF* locus in the 9p21 region. Below are H3K4me3, H3K27ac (enhancers), PolII, CTCF, mNET-seq tracks, GRO-seq tracks, PRO-seq tracks and gene annotations. The highlighted region shows the B1, B2 and B3 CTCF sites at the 3' boundary and super-enhancer. **B**. Browser shot showing the zoomed-in region of the 3' boundary (B1 and B2 CTCF sites). Below are H3K27ac, H3K4me1, H3K4me2, PolII, CAGE seq tracks, mNET-seq tracks and CTCF peaks. Arrowheads at the bottom show CTCF motif orientation at the B1 and B2 CTCF sites.

A

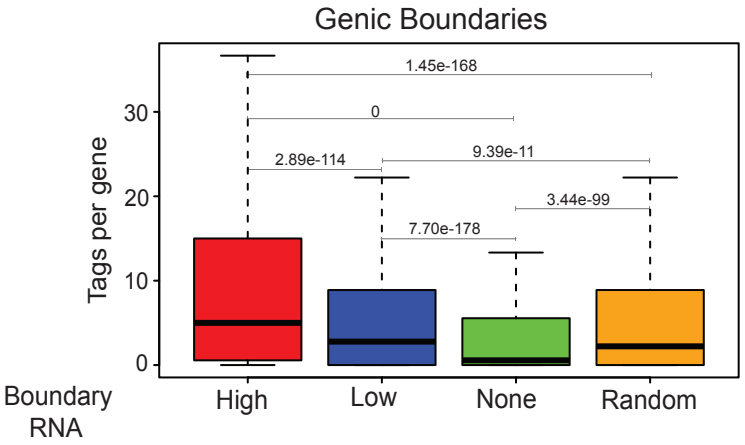

B

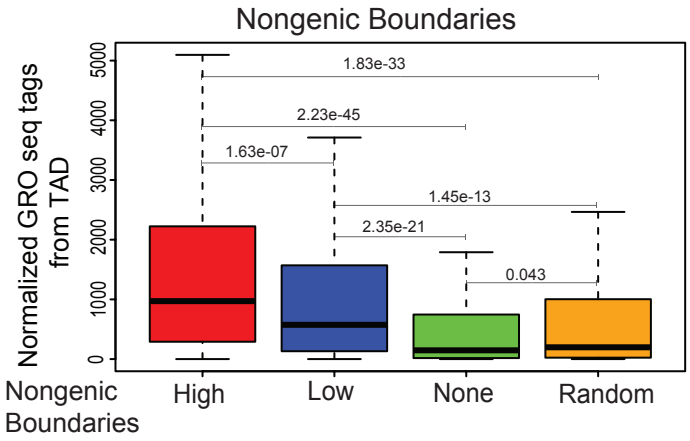

Supplemental Fig S7

Supplemental Fig S7. TAD transcription is correlated with transcribed boundaries: A. Box plots showing the normalized GRO-seq reads per gene within TADs of high, low, non-transcribed and random boundaries. **B.** Box plots showing the normalized GRO-seq tags within the TADs of transcribed nongenic boundaries with high and low boundary RNAs, non-transcribed and random boundaries.

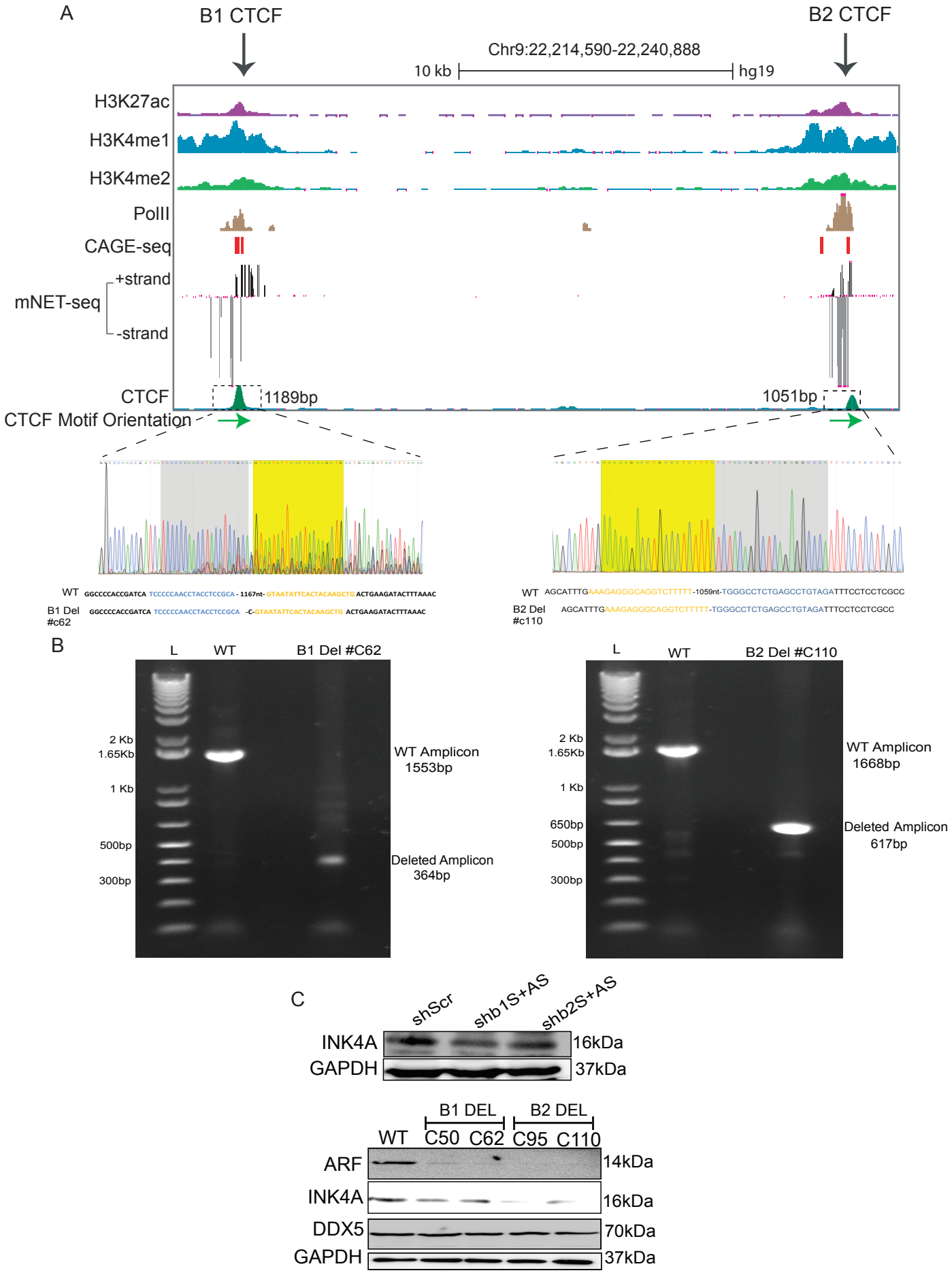

Supplemental Fig S8

Supplemental Fig S8. Deletion of B1 and B2 CTCF sites in the *INK4a/ARF* TAD boundary: A. UCSC Genome Browser track depicting the deleted B1 and B2 CTCF sites (boxed region at the bottom). Below are CAGE, NET-seq signal, CTCF peaks and CTCF orientation (Green arrows). The tracks zoom in to the chromatograms from Sanger sequencing on deleted amplicons to verify the deletion. **B.** Agarose gel images showing the amplicons from a Surveyor assay of B1 and B2 deletions. **C.** Immunoblot showing the protein levels of INK4A after shScr, shRNA knockdown against sense and anti-sense RNA at B1 and B2 CTCF sites (Upper panel). Immunoblot showing the protein levels of ARF, INK4A, DDX5 and GAPDH in WT and in cells with B1 and B2 CTCF site deletions (Lower panel).

A

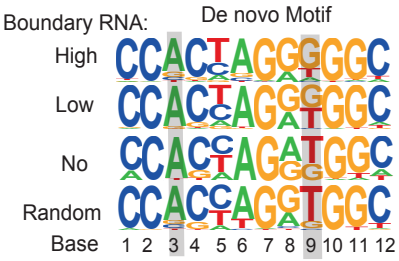

JASPAR CTCF Motif

Boundary RNA	P-value	log P-pvalue	% of Targets	% of Background	Match to CTCF (Jaspar) Motif
High	1e-175	-4.052e+02	46.85%	3.21%	0.90
Low	1e-253	-5.839e+02	61.72%	1.54%	0.92
No	1e-195	-4.498e+02	63.16%	1.60%	0.90
Random	1e-161	-3.724e+02	50.34%	2.13%	0.88

B

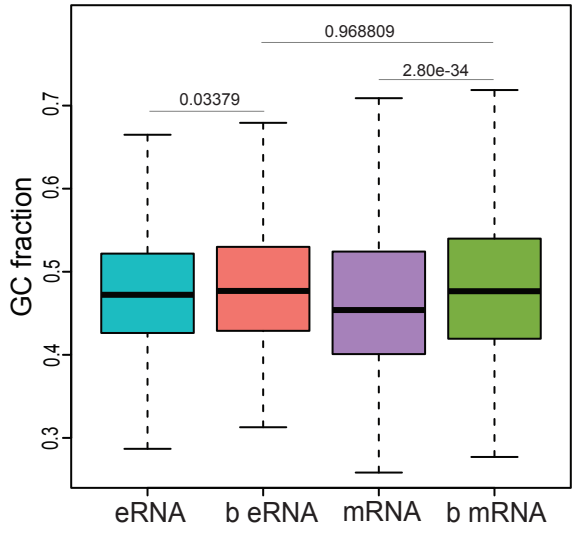

C

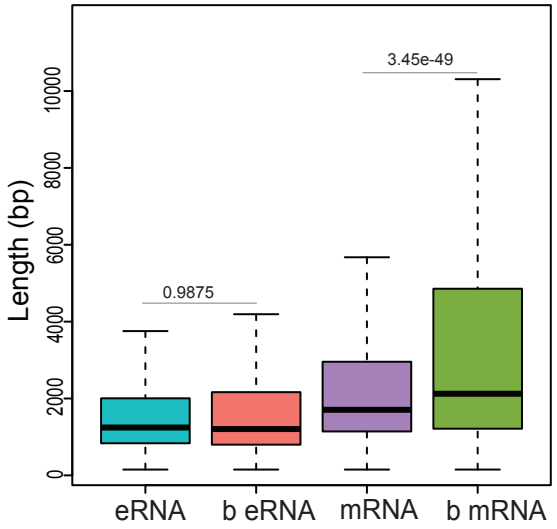

D

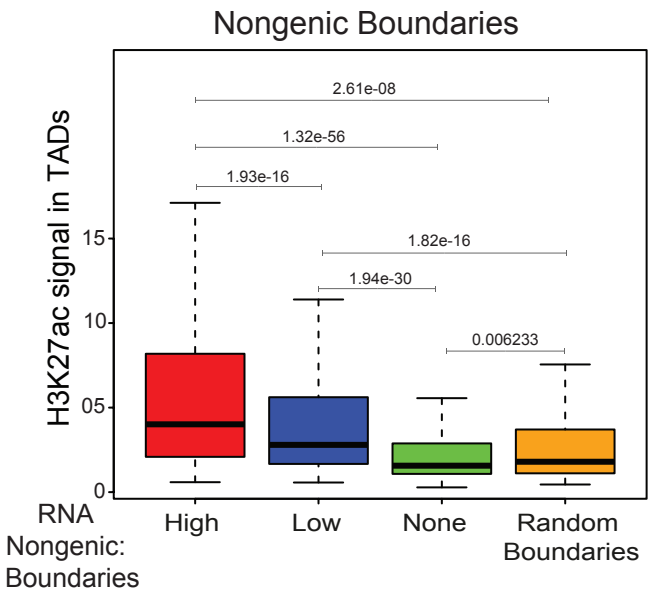

E

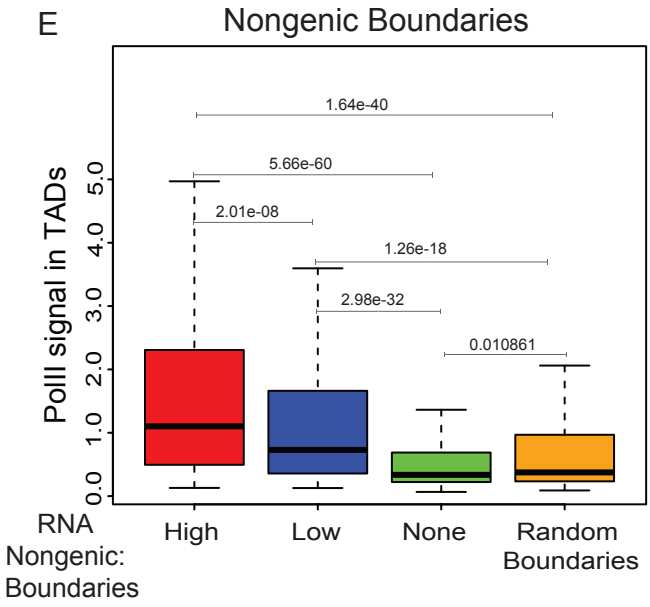

Supplemental Fig S9

Supplemental Fig S9. TADs with transcribed boundaries harbor more active enhancers: A. De novo and JASPAR motifs on boundaries with high, low, none RNA and random boundaries**.B.** Boxplots displaying the GC % of the transcripts identified as eRNA, boundary eRNA, mRNA and boundary mRNA. **C.** Boxplots displaying the Length of GRO-seq transcripts identified as eRNA, boundary eRNA, mRNA and boundary mRNA. **D.** Boxplots displaying enrichment of H3K27ac in TADs with high and low transcribed nongenic HeLa boundaries versus non-transcribed and random boundaries. **E.** Levels of PolII in TADs with different nongenic transcribed boundaries vs. non-transcribed and random boundaries.

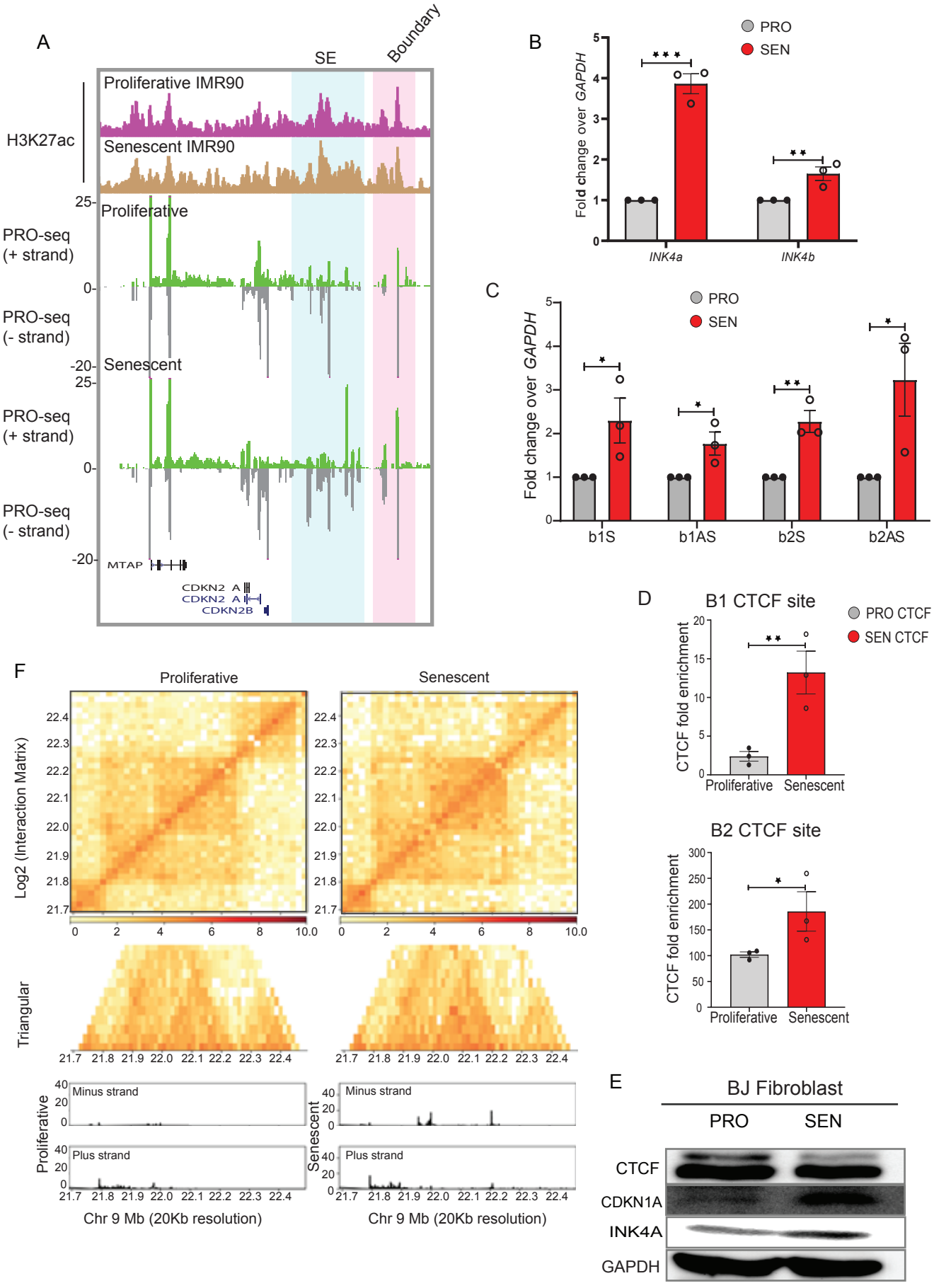

Supplemental Fig S10

Supplemental Fig S10. Transcriptional state of *INK4a/ARF* TAD in senescence : A. Browser images showing H3K27ac, PRO-seq reads on *INK4a/ARF* TAD from young and replicative senescent IMR-90 fibroblasts. Highlighted regions depict the super-enhancer and the boundary. **B**. qRT-PCR plots show the fold change in expression of *INK4a* and *INK4b* in young and DNA damage-induced senescent BJ fibroblasts. **C.** qRT-PCR plots show the fold change in expression of boundary RNA from B1 and B2 CTCF sites in young and DNA damage-induced senescent BJ fibroblasts. **D.** ChIP qRT-PCRs showing the changes in fold enrichment of CTCF at B1 and B2 CTCF sites in young and DNA damage-induced senescent BJ fibroblasts. Error bars denote SEM from three biological replicates. *p*-values were calculated by Student's two-tailed unpaired *t*-test in **B**, **C**, and **D .** $***p < 0.001$, $**p < 0.01$, $*p < 0.05$, $^{ns}p > 0.05$. **E.** Immunoblot showing the changes in protein levels of CTCF, CDKN1A, INK4A and GAPDH in young and DNA damage-induced senescent BJ fibroblasts. **F.** *INK4a/ARF* TAD structure in proliferating and senescent cells. Lower boxes represent the transcriptional levels.

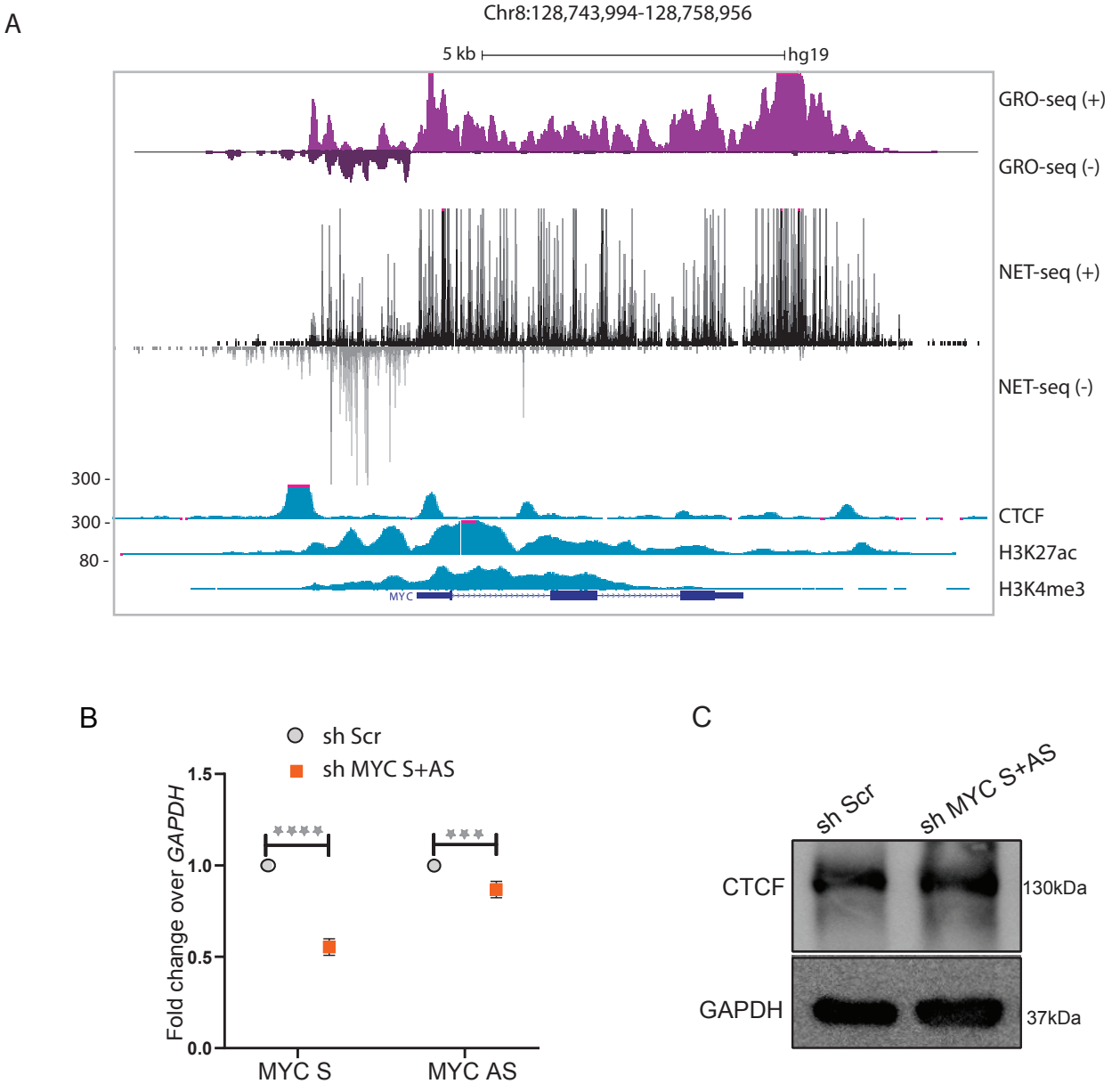

Supplemental Fig S11

Supplemental Fig S11. Browser shot of the *MYC* locus on 8q24 region: A browser shot showing the MYC locus on 8q24 region. GRO-seq, mNET-seq tracks, CTCF, H3K27ac, H3K4me3 and gene annotations are shown on the locus. **B.** qRT-PCRs showing the levels of sense and antisense RNA from *MYC* gene upon their shRNA mediated knockdowns**. C.** Immunoblot showing the CTCF levels upon *MYC* knockdown by the pool of shRNAs. Error bars denote SEM from three/four biological replicates. *p*-values were calculated by Student's two-tailed unpaired *t*-test in **B.** $****p < 0.0001$ $***p < 0.001$.